



**U.S. Army
Research Institute of
Environmental Medicine**

Natick, Massachusetts

**TECHNICAL REPORT NO. T20-05
DATE March 2020**

**ASSESSMENT OF EVAPORATIVE HEAT FLUX THROUGH WICKING FABRICS
USING A SWEATING GUARDED HOT PLATE**

Approved for Public Release; Distribution is Unlimited

United States Army
Medical Research & Development Command

DISCLAIMER

The opinions or assertions contained herein are the private views of the author(s) and are not to be construed as official or reflecting the views of the Army or the Department of Defense. The investigators have adhered to the policies for protection of human subjects as prescribed in 32 CFR Part 219, Department of Defense Instruction 3216.02 (Protection of Human Subjects and Adherence to Ethical Standards in DoD-Supported Research) and Army Regulation 70-25.

USARIEM TECHNICAL REPORT T20-05

**ASSESSMENT OF EVAPORATIVE HEAT FLUX THROUGH WICKING FABRICS
USING A SWEATING GUARDED HOT PLATE**

Alexander P. Welles ¹
Adam W. Potter ¹
Timothy P. Rioux¹
Larry G. Berglund ^{1,2}
Gabrielle A. Biby ²
Julio A. Gonzalez ¹
David P. Looney ¹
Xiaojiang Xu ¹

¹Biophysics and Biomedical Modeling Division, U.S. Army Research Institute of
Environmental Medicine, Natick, MA 01760

² Oak Ridge Institute for Science and Education (ORISE), Oak Ridge, TN, 37830

March 2020

U.S. Army Research Institute of Environmental Medicine
Natick, MA 01760-5007

REPORT DOCUMENTATION PAGE

*Form Approved
OMB No. 0704-0188*

The public reporting burden for this collection of information is estimated to average 1 hour per response, including the time for reviewing instructions, searching existing data sources, gathering and maintaining the data needed, and completing and reviewing the collection of information. Send comments regarding this burden estimate or any other aspect of this collection of information, including suggestions for reducing the burden, to Department of Defense, Washington Headquarters Services, Directorate for Information Operations and Reports (0704-0188), 1215 Jefferson Davis Highway, Suite 1204, Arlington, VA 22202-4302. Respondents should be aware that notwithstanding any other provision of law, no person shall be subject to any penalty for failing to comply with a collection of information if it does not display a currently valid OMB control number.

PLEASE DO NOT RETURN YOUR FORM TO THE ABOVE ADDRESS.

1. REPORT DATE (DD-MM-YYYY)		2. REPORT TYPE		3. DATES COVERED (From - To)	
4. TITLE AND SUBTITLE				5a. CONTRACT NUMBER	
				5b. GRANT NUMBER	
				5c. PROGRAM ELEMENT NUMBER	
6. AUTHOR(S)				5d. PROJECT NUMBER	
				5e. TASK NUMBER	
				5f. WORK UNIT NUMBER	
7. PERFORMING ORGANIZATION NAME(S) AND ADDRESS(ES)				8. PERFORMING ORGANIZATION REPORT NUMBER	
9. SPONSORING/MONITORING AGENCY NAME(S) AND ADDRESS(ES)				10. SPONSOR/MONITOR'S ACRONYM(S)	
				11. SPONSOR/MONITOR'S REPORT NUMBER(S)	
12. DISTRIBUTION/AVAILABILITY STATEMENT					
13. SUPPLEMENTARY NOTES					
14. ABSTRACT					
15. SUBJECT TERMS					
16. SECURITY CLASSIFICATION OF:			17. LIMITATION OF ABSTRACT	18. NUMBER OF PAGES	19a. NAME OF RESPONSIBLE PERSON
a. REPORT	b. ABSTRACT	c. THIS PAGE			19b. TELEPHONE NUMBER (Include area code)

<u>Section</u>	<u>Page</u>
List of Figures.....	iii
List of Tables.....	iii
Acknowledgments	iv
Executive Summary	1
Introduction	2
Methods	3
Materials	3
Fabric Thickness and Density	3
Thermal and Evaporative Resistance	3
Thermal Resistance.....	4
Evaporative Resistance.....	4
Evaporative Potential.....	5
Wicking	5
Evaporative Heat Flux.....	5
Results	7
Wicking and Thermal Properties.....	8
Evaporative Heat Flux.....	9
Discussion	12
Conclusions	13
References.....	14

LIST OF FIGURES

<u>Figure</u>		<u>Page</u>
1	Sweating guarded hot plate experimental apparatus with water bladder and delivery system.	6
2	Scanning electron microscope (SEM) images at 100X magnification of inward “skin” face (left), and outward face (right) for fabric structure (samples A-F).	8
3	Averaged evaporative heat flux profiles for all fabrics and bare plate	10
4	Linear regression of i_m/clo plotted against peak evaporative heat flux	11

LIST OF TABLES

<u>Table</u>		<u>Page</u>
1	Fabric sample designation (A-F), manufacturer and model, fabric fiber content, textile structure, average thickness, and average density.	7
2	Longitudinal wicking test results: average percent mass change, average height water wicked, and the product of wicking height and percent mass change for fabric samples A-F.	8
3	Fabric dry (R_t) and evaporative (R_{et}) thermal resistances and permeability (i_m) values as determined by sweating guarded hot plate	9
4	Total heat flux mean, standard deviation, confidence intervals, absolute error, and coefficients of variance for each fabric and bare plate	9
5	Peak evaporative heat flux after application of one milliliter of water	11

ACKNOWLEDGMENTS

Special thanks to Mr. William Tharion for his editorial assistance, Mr. David Ziegler for operating the scanning electron microscope, and Dr. Reed Hoyt for his continued mentorship and initially suggesting the use of the sweating guarded flat plate for wicking analyses.

EXECUTIVE SUMMARY

This study details a technique for comparing the evaporative capacity of fabrics. A Sweating Guarded Hot Plate (SGHP) was used to measure peak evaporative heat flux. In addition to the method we introduce, two commonly-used moisture transfer tests were performed for comparison, a longitudinal wicking “strip” test, and ASTM F1868-17 SGHP analysis of evaporative resistance. Thermal resistance was also measured on the SGHP. Results: The evaporative heat flux test was able to distinguish heat transfer differences between the six fabrics tested with peak rates ranging from 75 and 143 W/m². The mean absolute error between observed and expected results was 3.4 ± 5.9% with a coefficient of variation of 4.5% across all tests. The peak heat flux rate was moderately correlated to the “evaporative potential”, (i_m/clo) of each fabric ($R = 0.63$) but was not correlated with longitudinal wickability as determined by wicking strip test ($R = -0.06$). While more research is needed to establish best practices for the evaporative heat flux test, it appears useful for distinguishing unique heat transfer properties of fabrics.

INTRODUCTION

Evaporative heat flux through textiles provides a basis for comparing materials and clothing ensembles in terms of their evaporative potential. This is especially relevant given the increasing number of commercial “performance fabrics” specifically designed to wick moisture from the skin to facilitate evaporation. Success of wicking fabrics as consumer products is due in part to their effectiveness to benefit the individual in extreme environments or conditions. In cold weather conditions, wicking fabrics enable the transport of moisture away from the skin keeping the body drier and, by virtue of dry air’s insulative properties, warmer. During hot weather activities, wicking fabrics allow for transport of sweat through a garment and distribute it over a larger surface, resulting in greater evaporative cooling and potential for increased relief from heat strain. However, due to the complex nature of textile structures and the physics of fluid transfer through such mediums, it remains difficult to quantify the rate at which fabrics wick fluid and the amount of evaporative heat loss this wicking confers. Additionally, there is a lack of a widely accepted standard test method as well as varied definitions of wickability testing.

In general, textiles designed to mitigate heat strain via evaporative cooling do so by increasing the surface area over which sweat spreads thereby increasing the surface area over which evaporation may occur. This is accomplished through the physical mechanism of wicking, i.e., the movement of liquid moisture along the surface of fibers without being absorbed by those fibers [1]. The wicking effect is particularly important considering that sweat rate is not uniform across the skin’s surface [2]. Fluid transport along fabric fibers is mediated by capillary forces at work between a fluid and the fabric’s structure [3]. In addition to “wickability,” the phenomenon of “wettability,” i.e., the relative ease with which the fabric-air interface is replaced with a fiber-liquid-air interface when the fabric is initially exposed to moisture [4], is an important determinant of the rate at which a fabric will transport moisture [5-6]. Various tests are used to measure the rate at which a fabric wicks and/or wets but not all researchers make a distinction between the two processes [6] or relate wicking rate to evaporative heat flux or heat loss. However, it is generally accepted that a fabric’s ability to wick is determined by its capillarity [7-10] which, in turn, is determined by the combination of the attractive forces between the liquid and its surroundings (adhesion) and intermolecular attractive forces between the liquid’s own molecules (cohesion).

Because of the complexity involved in modeling the adhesive and cohesive kinetics between a fluid and a porous textile, it would be useful to develop a quantitative method by which the evaporative rate of water from a fabric can be determined directly without, per se, measuring textile wickability or wettability. Evaporative cooling and drying time can be measured on a thermal manikin [11] but require the fabrication of a fully wearable garment or ensemble. The use of a Sweating Guarded Hot Plate (SGHP) allows a fabric to be evaluated more easily and with less work than fabricating a full garment for test purposes. A test methods exists for measuring drying time of a fabric on a heated plate, but does not utilize heat flux or peak heat flux [12]. The present effort explores the use of a SGHP to measure the rate of evaporative heat flux in comparison

to two standard methods of assessing moisture transfer through textiles, (a) the longitudinal wicking “strip” test [4] and, (b) analysis of evaporative resistance by SGHP [13]. Six wicking fabric samples were examined and three repeated tests on each fabric were performed in order to determine the heat flux properties of each fabric and whether peak evaporative heat flux correlates with direct assessments of wickability and water vapor permeability.

METHODS

Materials

Six fabrics were assessed in this study. Of the six samples (labeled A to F), five are commercially marketed as fabrics designed to wick moisture away from the skin and distribute it evenly to facilitate comfort and evaporation. Fabric A was cut from a men’s Under Armour T-shirt (Tech Longsleeve, Under Armour, Baltimore, MD); fabric B through E were Powerdry (Polartec LLC, Lawrence, MA) styles 7502, 9042, 2014, 9049 respectively. Fabric C is currently used as the base layer in the Extended Cold Weather Clothing System (ECWCS) GEN III and style 2014 is the torso fabric for the Special Forces Level 9 Combat Shirt. The sixth fabric (F) was cut from a new men’s 100% cotton undershirt (Hanes TAGLESS T-Shirt H5250, Hanesbrands Inc., Winston-Salem, NC). Fabric fiber content and structure are listed in Table 1. Fabrics C, D, and E received the same proprietary Polartec chemical wicking treatment during production (personal communication, Polartec) but it is unknown if A, B, and D received any wicking treatment.

The knit structures of the fabric samples were imaged using a scanning electron microscope (SEM) (Carl Zeiss SMT Model EVO 60; Carl Zeiss Microscopy, LLC; Thornwood, NY) equipped with an energy dispersive X-ray spectrometer (EDS) (Genesis model EDS; EDAX, Inc.; Mahwah, NJ) at the Combat Capabilities Development Command Soldier Center, Natick, MA. Samples were cut to roughly ~1 x 0.5 cm and sputter coated with about 17 nm Au/Pd for imaging. Images were made at magnifications of 100, 250, 500, and 1000X.

Fabric Thickness and Density

Each fabric’s thickness was measured with a dial thickness gauge (MTG-DX2 Digital Contact Material Thickness Gauge, Electromatic Equipment Co., Cedarhurst, NY) according to ASTM D1777-96 standards [14].

Thermal and Evaporative Resistance

Thermal and evaporative resistances were measured using a Sweating Guarded Hot Plate (Model 306-200/400, Thermetrics, Seattle, WA) under ASTM F1868-17 conditions (“dry” thermal resistance test conditions—hotplate surface temperature 35°C; environmental chamber: 65% relative humidity (RH), 20°C ambient air temperature (T_a), 1.0 m/s wind speed. “wet” evaporative resistance conditions—hotplate temperature 35°C; environmental chamber: 40% RH, 35°C T_a , 1.0 m/s wind speed) [13] with the

manufacturer specified outward face of the fabric facing up (towards the environment) and the inward facing “skin” side against the SGHP.

Thermal Resistance

Thermal resistance was calculated in SI units from:

$$R_t = \frac{(T_s - T_a)}{Q/A} [\text{m}^2 \cdot \text{°C}/\text{W}] \quad \text{Eq 1.}$$

where R_t is the total thermal resistance ($\text{m}^2 \cdot \text{°C}/\text{W}$) of the fabric and boundary air layer, T_s is the hotplate average temperature (°C), T_a is the ambient chamber air temperature (°C), and Q/A is the heat flux (W/m^2). The intrinsic thermal resistance of the fabric is calculated by:

$$R_{cf} = R_t - R_{cbp} [\text{m}^2 \cdot \text{°C}/\text{W}] \quad \text{Eq 2.}$$

where R_{cf} is the intrinsic thermal resistance of the fabric ($\text{m}^2 \cdot \text{°C}/\text{W}$) and is calculated by subtracting the bare plate resistance R_{cbp} ($\text{m}^2 \cdot \text{°C}/\text{W}$) from the total thermal resistance R_t . Thermal resistance (insulation) is often provided in units of clo, which is defined as the insulation required to keep a resting man comfortable at 21°C and air movement of 0.1 m/s [13]. The clo equivalency to SI units of thermal resistance is shown in Equation 3.

$$1 \text{ clo} = 0.155 [\text{m}^2 \cdot \text{°C}/\text{W}] \quad \text{Eq 3.}$$

Evaporative Resistance

The total evaporative resistance of the fabric and the boundary air layer was calculated in SI units using:

$$R_{et} = \frac{(P_{sat} - P_{amb})}{Q/A} [\text{m}^2 \cdot \text{Pa}/\text{W}] \quad \text{Eq 4.}$$

where R_{et} ($\text{m}^2 \text{Pa}/\text{W}$) is the total evaporative resistance, P_{sat} is the saturation vapor pressure (Pa) at the hotplate surface temperature, P_{amb} is the ambient vapor pressure (Pa). The intrinsic evaporative resistance of the fabric was calculated by:

$$R_{ef} = R_{et} - R_{ebp} [\text{m}^2 \cdot \text{Pa}/\text{W}] \quad \text{Eq 5.}$$

where R_{ef} is the intrinsic evaporative resistance of the fabric ($\text{m}^2 \cdot \text{Pa}/\text{W}$) and R_{ebp} is the bare plate evaporative resistance ($\text{m}^2 \cdot \text{Pa}/\text{W}$). The dimensionless permeability index is calculated using equation 6 and has a range from 0 to 1, 0 being completely impermeable and 1 being the greatest theoretical permeability. Note that R_t must be in SI units [$\text{m}^2 \cdot \text{°C}/\text{W}$]

$$i_m = \frac{60.6515 \cdot R_t}{R_{et}} \quad [\text{N.D.}] \quad \text{Eq 6.}$$

Evaporative Potential

The values of R_t can be converted to measures of total thermal insulation (I_T) in units of clo, a water vapor permeability index (i_m), and a ratio of these two parameters are typically used to describe an ensemble's evaporative potential (i_m/clo) [14-17]. In this case we have applied the use specific to just a textile; while we recognize the importance for distinguishing between the two [18].

Wicking

The longitudinal wicking "strip" test, also called the Determination of the Rate of Absorption of Water by Textile Materials (Height of Rise Method), from DIN 53924 [19] was used to compare each fabric's wicking capacity. A 2.54 cm by 15.24 cm strip was cut from each material and suspended lengthwise with the lower tip immersed 1 cm in a beaker of distilled water in a controlled environment of 20°C and 65% relative humidity (RH). After one minute, the height reached by the water in the fabric was recorded by observing the fabric in front of a light source. A total of three measurements were made for each fabric and average heights of rise are listed in Table 1. Initial and final masses were measured using an Ohaus Explorer Pro EP4102 Precision Balance (Ohaus, Nanikon, Switzerland). The product of height of rise and percent mass increase of fabric was calculated to provide a basis for comparison of mass transfer rates and wicking distance [6,20].

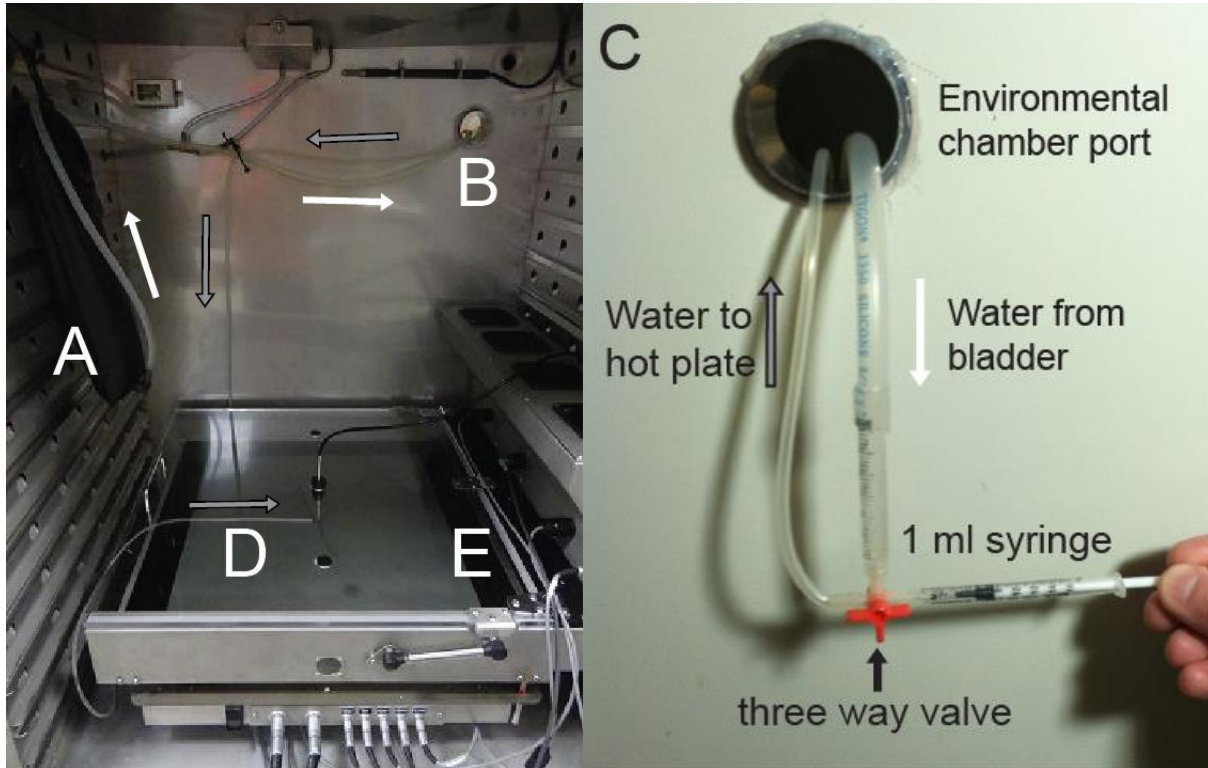
Evaporative Heat Flux

Measurement of Evaporative Heat Flux

The SGHP was used to determine each fabric's evaporative heat flux properties. 1 ml of isothermal distilled/deionized water was applied to the center of each 40.64 square cm fabric sample. The environmental conditions from evaporative resistance measurements (Procedure Part B) of ASTM F1868-17 were used for each test (T_a : $35 \pm 0.5^\circ\text{C}$ with $< \pm 0.1^\circ\text{C}$ fluctuation, air velocity: 0.5 - 1.0 m/s with ± 0.1 m/s fluctuation, RH: $40 \pm 4\%$, T_s : $35 \pm 0.1^\circ\text{C}$). The SGHP was not sweating for these measurements and no cellophane was placed between the fabric and SGHP as is done for evaporative resistance tests following the ASTM standard. The fabric sample was rolled onto the SGHP uniformly to minimize stretching and provide consistent contact (minimize air gaps) as per the ASTM standards.

Prior to adding water to the system, heat flux measurements are approximately constant because the plate and environment are in thermal equilibrium ($T_a = T_s$). Once water is introduced to the system the heat flux rises. Heat flux data were recorded each minute from when water was introduced until a return to zero or near zero heat flux was recorded. This procedure was repeated three times for each sample. In addition to adding 1 ml to each fabric sample, three repetitions of adding 1 ml to the hot plate alone were performed to provide a baseline comparison. Figure 1 shows the experimental setup to deliver the 1 ml of water to the fabric. The volume of 1 ml was chosen to simplify calculations and avoid water migrating outside the fabric boundary and the test plate portion of the hot plate.

Figure 1. Sweating guarded hot plate experimental apparatus with water bladder and delivery system. A: water bladder, B: external access port leading to three way valve and syringe, C: external syringe and three-way valve, D: tubing delivering water aliquot to SGHP, and E: fan output creating airflow from right to left.



Note: white arrows indicate flow of water from bladder to syringe and grey arrows indicate flow of water from syringe to SGHP.

The collapsible bladder used to provide the water for the test was housed within an environmental chamber (Model CEO0932-4, Lunaire Steady State/Stability Test Chamber, Thermal Product Solutions, New Columbia, PA) to ensure that water delivered to the SGHP for evaporation was isothermal with the chamber and hot plate. This necessitated running tubing to an external access port where a three way valve was used to allow a 1 mL syringe to draw measured volumes of isothermal water from the bladder and expel them through the tubing onto the center of the fabric and hot plate. The water expelled during a trial was contained in roughly the first 5 cm of the tube labeled B in Figure 1. Thus, great care was taken to ensure no bubbles were present in the delivery tube prior to or during the 1ml delivery. The delivery tube was placed on top of the fabric sample parallel to the fan output in order to limit its disturbance of laminar air flow. The tube was also centered on the test plate in order to limit the possibility that the liquid delivered would wick onto the guard plate. The syringe plunger was depressed evenly over the course of 2 seconds to avoid forcing the water out over irregular surface areas for each trial.

Calculation of Evaporative Heat Flux

The hot plate control software (Thermdac v8.1.12.0, Thermetrics; Seattle, WA) recorded minute averages of the heat flux across the test plate portion of the SGHP. The conversion from heat flux (W/m^2) to total joules of energy expended to maintain the test plate's temperature as water evaporated was calculated as follows:

$$E [J] = \sum \left(\frac{Q}{A} [W/m^2] \cdot A [m^2] \cdot t [s] \right) \quad \text{Eq. 8}$$

where 0.065 m^2 is the area of the test plate portion of the SGHP (25.4 cm by 25.4 cm) and 60 s was the period over which the SGHP averaged heat flux.

The total evaporative heat transfer was calculated using the expected energy requirement to evaporate 1 ml of 35°C water. Per ASHRAE handbook, at 35°C , the specific enthalpy of evaporation for water is 2417.94 J/g [21]. Results measuring in excess of $\pm 10\%$ of the known enthalpy of evaporation for water at 35°C were discarded as erroneous. Drying times were calculated as the time it took for heat flux to return to a steady state baseline observed for 30 minutes prior to water application.

RESULTS

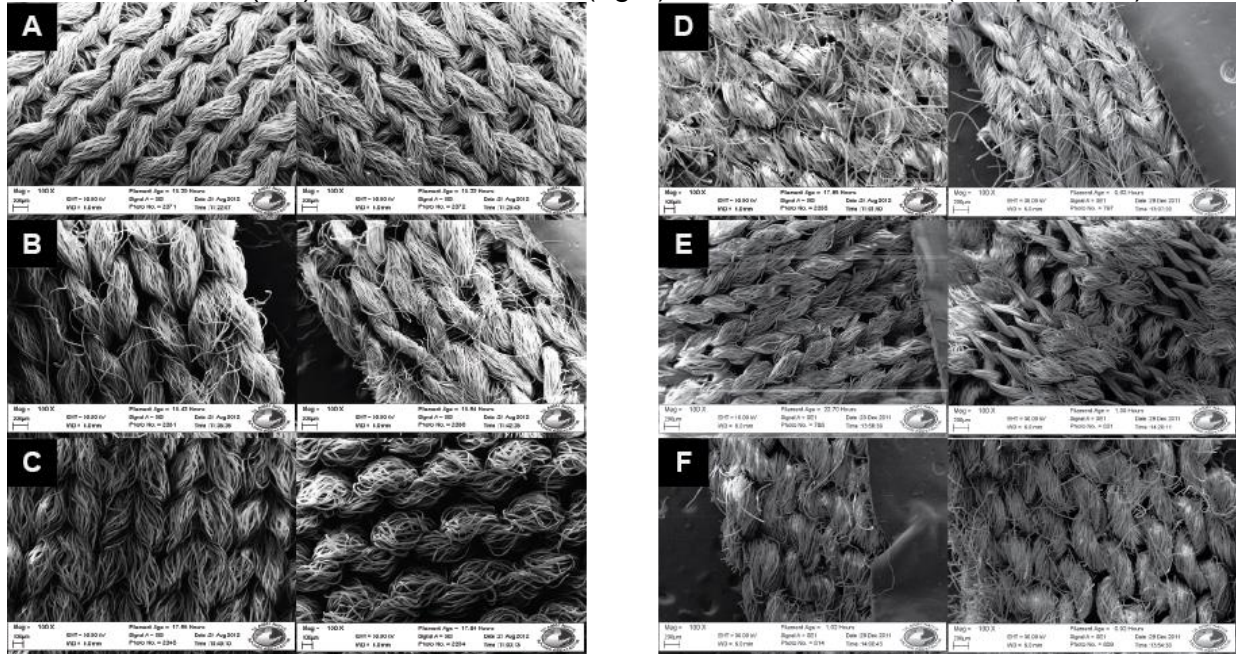
Textile thickness and density are shown in Table 1.

Table 1. Fabric sample designation (A-F), manufacturer and model, fabric fiber content, textile structure, average thickness, and average density.

Fabric	Manufacturer and Model	Fiber content	Fabric Structure	Average thickness (mm)	Average density (g/cm^3)
A	UA Tech Longsleeve T-shirt	100% polyester	knit	0.46	3.40
B	Polartec Powerdry Style 7502	100% polyester	knit	0.74	3.92
C	Polartec Powerdry Style 9042	100% polyester	knit	0.58	4.18
D	Polartec Powerdry Style 2014	68% modacrylic, 29% rayon, 3% spandex	knit	0.51	2.66
E	Polartec Powerdry Style 9049	100% polyester	knit	0.61	4.24
F	Hanes H5250 cotton t-shirt	100% cotton	knit	0.42	2.80

Figure 2 shows images at 100X magnification of the knit structure for each fabric's inward facing "skin" side and outward facing surface side.

Figure 2. Scanning electron microscope (SEM) images at 100X magnification of inward “skin” face (left), and outward face (right) for fabric structure (samples A-F).



Wicking and Thermal Properties

Table 2 presents the results of the wicking strip test and gives values for average percent mass change, average height water wicked, and the product of wicking height and percent mass change. Table 3 provides the results of the SGHP testing and gives each fabrics’ results for thermal and evaporative resistance measurements as well as calculated i_m values.

Table 2. Longitudinal wicking test results: average percent mass change, average height water wicked, and the product of wicking height and percent mass change for fabric samples A-F.

Fabric	Mass change (%)	Average wicking height (cm)	(Wicking height • % mass change) /100
A	217.3	7.90	17.17
B	230.6	6.87	15.83
C	202.5	6.47	13.10
D	199.1	7.10	14.14
E	222.2	4.30	9.55
F	203.5	4.57	9.29

Table 3. Fabric dry (R_t) and evaporative (R_{et}) thermal resistances and permeability (i_m) values as determined by sweating guarded hot plate.

Fabric	R_t ($m^2 \cdot ^\circ C \cdot W^{-1}$)	R_{cf} ($m^2 \cdot ^\circ C \cdot W^{-1}$)	R_t (Clo)	R_{et} ($m^2 \cdot Pa \cdot W^{-1}$)	R_{ef} ($m^2 \cdot Pa \cdot W^{-1}$)	i_m	i_m/clo
A	0.080	0.010	0.516	7.928	3.928	0.614	1.191
B	0.101	0.031	0.652	10.348	6.306	0.588	0.902
C	0.080	0.010	0.513	7.961	3.961	0.610	1.189
D	0.103	0.033	0.661	9.629	5.629	0.645	0.976
E	0.082	0.012	0.530	8.040	4.040	0.620	1.171
F	0.081	0.011	0.520	8.973	4.973	0.547	1.051

Note: higher i_m/clo = better evaporative potential. 1 clo = 0.155 $m^2 \cdot ^\circ C/W$. R_t is total thermal resistance, R_{cf} is intrinsic thermal resistance of the fabric, R_{et} is total evaporative resistance, and R_{ef} is intrinsic evaporative resistance of the fabric.

Evaporative Heat Flux

Table 4 presents mean and standard deviations for the total joules of energy required to evaporate 1ml of water for each fabric sample and the bare plate as determined by return of heat flux to baseline values. Percent absolute error was calculated by taking the difference between the average total joules measured and the specific enthalpy of water at 35°C (2417.94 J/g) and multiplying by 100. The 95% confidence interval (CI) and coefficient of variation (CV) are also reported (Table 4).

Table 4. Total heat flux mean, standard deviation, confidence intervals, absolute error, and coefficients of variance for each fabric and bare plate.

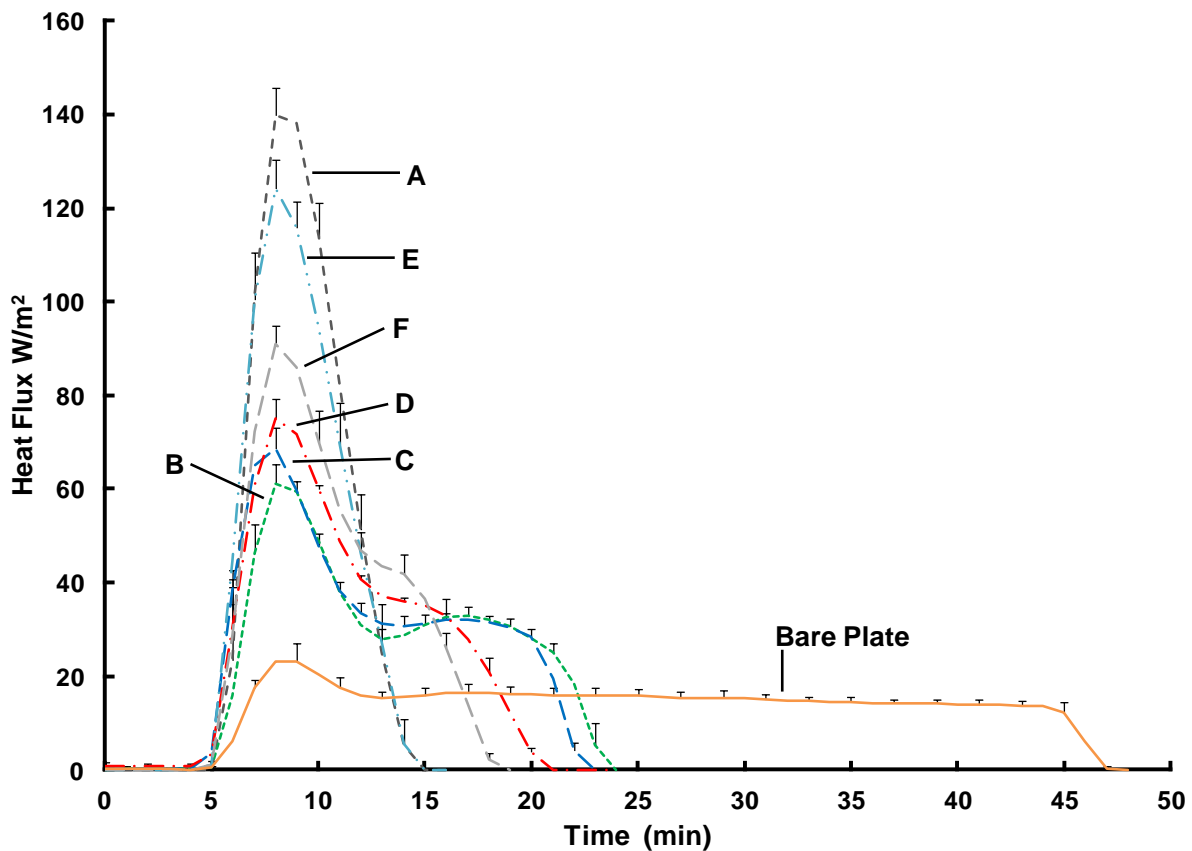
Fabric	Mean ± Standard Deviation (J)	±95% Confidence Interval (J)	Specific Enthalpy Mean diff (J)	Mean Absolute Error (J)	Mean Absolute Error ± Standard Deviation (%)	Coefficient of Variance (%)
A	2634.7 ± 72.8	42.0	82.4	216.8	9.0 ± 3.0	2.76
B	2297.6 ± 115.2	66.5	130.4	-120.3	5.0 ± 4.8	5.02
C	2423.7 ± 157.6	91.0	178.3	5.8	0.2 ± 3.3	6.50
D	2308.5 ± 85.6	49.4	96.8	-109.4	4.5 ± 3.5	3.71
E	2435.2 ± 83.0	47.9	93.9	17.3	0.7 ± 1.0	3.41
F	2382.7 ± 103.6	59.8	117.2	-35.2	1.5 ± 3.0	4.35
Bare Plate	2343.5 ± 130.6	75.4	147.7	-74.4	3.1 ± 5.4	5.57
All	2403.7 ± 142.8	31.2	61.1	-14.2	3.4 ± 5.9	4.47

Note: "Bare Plate" indicates no fabric was placed on the SGHP when the one milliliter aliquot of water was administered. The specific enthalpy of water at 35°C is 2417.94 J/g.

Figure 3 presents the evaporative heat flux values recorded every minute over time for each fabric sample and the bare wetted SGHP. The area under each curve corresponds to the total evaporative heat values in Table 4 which are approximately equal to the enthalpy of 1 mL of water at 35 °C, 2417.94 J.

Table 5 provides the peak evaporative heat flux values for all fabrics. Shortest drying times (10, 19, 18, 16, 10, 12, 42 min for fabrics A, B, C, D, E, F, and bare plate respectively) correlated with highest peak evaporative heat fluxes (Table 5) according to logarithmic ($R = 0.97$; $y = -18.32 \cdot \ln(x) + 96.908$) and power regression ($R = 0.99$; $y = 592.5 \cdot x^{0.839}$).

Figure 3. Averaged evaporative heat flux profiles for all fabrics and bare plate.



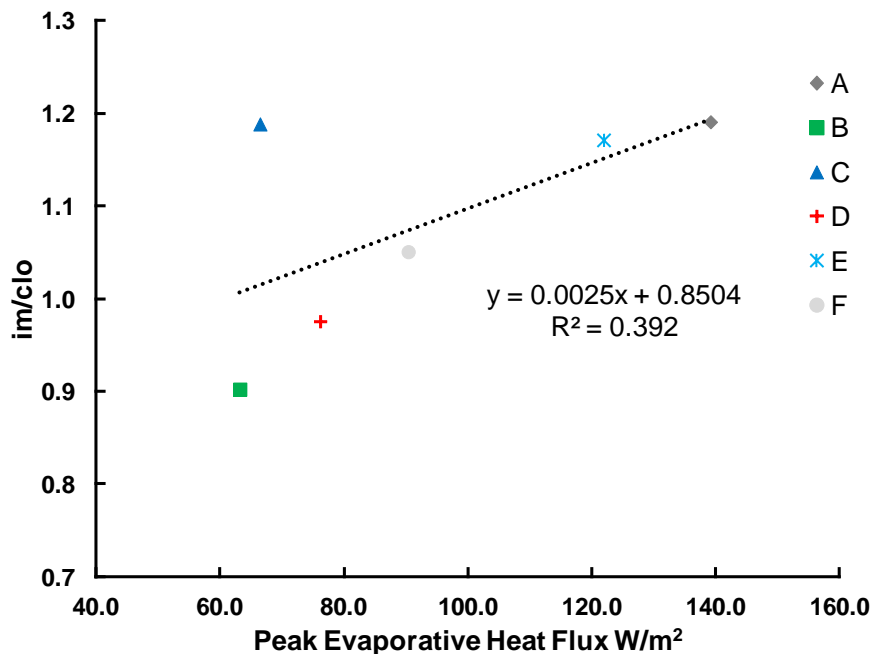
Note: error bars represent standard deviations and are only shown as positive values for clarity. Dry time is calculated by subtracting five minutes from the time at which evaporative heat flux returns to zero.

Table 5. Peak evaporative heat flux after application of one milliliter of water.

Fabric	Peak evaporative heat flux (W/m ²)				1ml dry time (min)
	trial 1	trial 2	trial 3	mean of trials ± 1 standard deviation	
A	135.5	142.9	151.7	143.4 ± 8.1	10
B	61.1	65.2	57.1	61.1 ± 4.1	19
C	69.2	63.7	72.7	68.5 ± 4.6	18
D	72.3	80.0	73.3	75.2 ± 4.2	16
E	116.8	127.2	120.9	121.6 ± 5.2	10
F	94.3	86.5	92.0	90.9 ± 4.0	12
Bare Plate	23.4	19.6	27.3	23.4 ± 3.8	42

There was a moderate correlation between the peak evaporative heat flux rates and the i_m/clo of each fabric ($R=0.63$, Figure 4). Interestingly, the removal of fabric C increased the R value for a linear fit line to $R = 0.99$. The fabrics' wicking height or the product of wicking height and percent mass change was unrelated to the peak evaporative heat flux of the fabrics, $R=-0.06$ and $R=-0.01$ respectively.

Figure 4. Linear regression of i_m/clo plotted against peak evaporative heat flux.



DISCUSSION

This work sought to determine whether the peak evaporative heat flux of 1 mL of isothermal water correlates with direct assessments of a fabric's wickability and water vapor permeability. The thermal properties of six wicking fabric samples and their heat flux responses to application of 1 mL of isothermal water were measured via SGHP. Wickability was assessed using a longitudinal strip wicking test. Of the measured results, i_m/clo correlated most strongly with peak evaporative heat flux with one clear outlier. The presence of this outlier may indicate that i_m/clo doesn't by itself adequately indicate a fabric's capacity for evaporative cooling.

A secondary observation is that the evaporative heat flux test is able to capture textile properties not revealed by wicking and i_m/clo determinations. While the fabric with the shortest dry time and greatest wicking height and i_m/clo had the greatest peak evaporative heat flux, this was not observed in the remaining samples. A general trend evident from Pearson correlation (Figure 4) revealed that i_m/clo contributed to some of the evaporative heat flux variation, whereas the wickability measures did not.

Correlation between peak evaporative heat flux and permeability appeared to be compromised by the test outcomes of fabric C, which possessed a high i_m/clo but a relatively low peak evaporative heat flux. Method of manufacture (e.g., woven versus non-woven), chemical treatment (e.g., sealants, repellants, and flame retardants), and material (synthetic versus natural) could all affect the relationship between permeability and evaporative heat flux. Despite different knits patterns (Figure 2), the densities for Fabrics B, C, and E (Table 1) were similar as were the fabric thicknesses. This might suggest that the knit structure played a key role in affecting evaporative heat flux. There were no clearly observed differences in wettability (e.g. requiring physical pressure to force liquid into the fabric) as each fabric immediately absorbed the 1 ml aliquot as it was administered. According to the manufacturer, fabric C received the same wicking treatment as fabrics D and E during manufacture.

Although scanning electronic microscope photographs clearly indicate differences in knit structure, it is difficult to draw concrete or quantitative conclusions from them. It may be possible that the knit structure of fabric C contributes to being an outlier for the correlation of peak evaporative heat flux and i_m/clo . For example, the relative tightness of fabric C's knit may effectively sequester more fluid in the center of the fabric than on either surface. Regardless, these outcomes indicate that no single test can capture all fabric properties, and additional tests using a variety of fabric types are needed to provide a deeper understanding of the complex relationship between fabric structure and evaporative heat transfer.

Although samples A and E were easily differentiated from the remaining samples by average peak evaporative heat flux values (143.4 and 121.6 W/m²); samples B, C, and D were closely grouped (61.1, 68.5, and 75.2 W/m²). The total evaporative heat flux recorded for all samples was within $\pm 10\%$ of 2417.94 J, indicating that the physical principles and procedures used for the measurements proved valid. The COV and low

mean absolute error values, as well as the ability to compare results to expected outputs, allow for this method of fabric evaporation to be reproduced with both precision and accuracy.

While the evaporative heat flux test appears promising for comparing the heat transfer properties of fabrics, further work is required to develop and refine the test methodology. Application of finite volumes of water (e.g., 1 ml, 10 ml, etc.) directly to the fabric provide insight into non-saturated peak evaporative heat flux. An alternative approach might be to let the fabric wick and saturate from an “infinite” liquid reservoir, thereby determining the maximal evaporative heat flux per surface area. It may also be informative to study the effects of fluid application at rates analogous to those of human sweat rate.

The role of air gaps, both between a fabric sample and the SGHP and within the fabrics, also needs to be better understood. For example, fabrics with raised portions or pilli trap air between themselves and the fabrics they abut against. This may affect the rate of evaporative heat flux as it reduces the area of physical contact between the fabric and the SGHP and introduces pockets of greater insulation. Other factors including chemical treatments, stitching patterns, and manufacturing processes may also affect the evaporative heat flux for a given textile. Therefore, the evaporative heat flux properties of well characterized fabrics should be tested to better understand the relationship between these factors and the potential for evaporative heat flux.

CONCLUSIONS

Measurement of peak evaporative heat flux with a SGHP appears to be a useful method for identifying the evaporative properties of fabrics. The methods described herein for measuring evaporative heat flux are based on rational principles, and are acceptably reproducible. Further tests are necessary, however, to better understand the impact of how the method of wetting the fabric, and physical properties of the fabric influence test outcomes.

REFERENCES

1. Tortora PH and Collier BJ. *Understanding Textiles*. Fifth edition. New York, NY: Prentice-Hall, pp. 41, 1997.
2. Patterson MJ, Galloway SDR, and Nimmo MA. Variations in regional sweat composition in normal human males. *Exp. Phys.*, 85(6): 869-75, 2000.
3. Hsieh Y-L. Liquid transport in fabric structures. *Textile Res. J.*, 65(5):299-307, 1995.
4. DIN 53924 German National Standard, 1997, "Testing of textiles—Velocity of soaking water of textile fabrics (method by determining the rising height)," Deutsches Institut für Normung e. V., Berlin, Germany, 1997.
5. Ghali K, Jones B, and Tracy J. Experimental techniques for measuring parameters describing wetting and wicking in fabrics. *Textile Res. J.*, 64(2):106-11, 1994.
6. Harnett PR and Mehta PN. A survey and comparison of laboratory test methods. *Textile Research Journal*, 54(7):471-8, 1984.
7. Kissa E. Wetting and wicking. *Textile Res. J.*, 66(10):660-8, 1996.
8. Nyoni AB and Brook D. Wicking mechanisms in yarns—the key to fabric wicking performance. *J. Textile Inst.*, 97(2):119-28, 2006.
9. Rajagopalan D, Aneja AP, and Marchal J-M. Modeling capillary flow in complex geometries. *Textile Res. J.*, 71(9):813-21, 2001.
10. Washburn EW. The dynamics of capillary flow. *Phys. Rev.*, 17(3):273-83, 1921.
11. Gonzalez RR, Breckenridge JR, Levell CA, Kolka MA, and Pandolf KB. Efficacy of Heat Exchange by Use of a Wettable Cover over Chemical Protective Garments. *Performance of Protective Clothing, ASTM STP 900*, Barker RL and Coletta GC, Eds., American Society for Testing and Materials, Philadelphia, pp. 515-34, 1986.
12. AATC TM201, -2014, "Drying Rate of Fabrics: Heated Plate Method," American Association of Textile Chemists and Colorists, Research Triangle Park, North Carolina, 2014.
13. ASTM Standard F1868, 2009, "Standard Test Method for Thermal and Evaporative Resistance of Clothing Materials Using a Sweating Hot Plate," ASTM International, West Conshohocken, PA, 2009.
14. Woodcock AH. Moisture transfer in textile systems, Part I. *Textile Research Journal*, 32(8), 628-633, 1962.

15. Woodcock AH. Moisture permeability index - A new index for describing evaporative heat transfer through fabric systems. Quartermaster Research and Engineering Command, Natick, MA 01702 USA, Technical Report (TR-EP-149), 1961.
16. Potter AW. Method for estimating evaporative potential (im/clo) from ASTM standard single wind velocity measures. US Army Research Institute of Environmental Medicine, Natick, MA, 01760, USA, Technical Report, T16-14, 2016, ADA#637325.
17. Potter AW, Gonzalez JA, Karis AJ, Santee WR, Rioux TP, and Blanchard LA. Biophysical characteristics and measured wind effects of chemical protective ensembles with and without body armor. US Army Research Institute of Environmental Medicine, Natick, MA, 01760, USA, Technical Report, T15-8, 2015. ADA#621169
18. Xu X, Rioux TP, and Potter AW. Fabric thermal resistance and ensemble thermal resistances are two different concepts. *Journal of Occupational and Environmental Hygiene*, 11(11), D187-188, 2014.
19. ASTM Standard D1777-96, 201, "Standard Test Method for Thickness of Textile Materials," ASTM International, West Conshohocken, PA, 2011.
20. Mehrtens DG and McAlister KC. Fiber Properties Responsible for Garment Comfort. *Textile Res. J.*, 32(8):658-65, 1962.
21. ASHRAE Handbook, Fundamentals. American Society of Heating, Refrigerating and Air-Conditioning Engineers, Inc. Atlanta, Georgia, pp. 1.6, 2009.